RSC Advances

ROYAL SOCIETY OF CHEMISTRY

www.rsc.org/advances

Journal Name

ARTICLE

Study on formation and properties of Al–Li–Sm alloy containing whiskers in molten salts

De−Bin Ji,[a] Yong−De Yan,[a,b,*] Mi−Lin Zhang,[a,*] Xing Li,[a] Xue Yang,[a] Xiao−Yan Jing,[a] Wei Han,[a] Yun Xue,[b] Zhi−Jian Zhang,[b] Thomas Hartmann[c]

Received 00th January 20xx,
Accepted 00th January 20xx

DOI: 10.1039/x0xx00000x

www.rsc.org/

The electrochemical behaviors of samarium ions on liquid aluminum electrode in LiCl–KCl melts at 973 K were investigated by the cyclic voltammetry, square wave voltammetry and cathodic polarization test. The results show that only one kind of Al–Sm intermetallic compound can be formed under our experiment condition. The Al–Li–Sm alloy containing whisker was obtained by galvanostatic electrolysis in LiCl–KCl melts after the addition of 10 wt. % $SmCl_3$ on liquid aluminum electrode at 973 K. The alloy containing whisker was characterized by X–ray diffraction (XRD) and scanning electron microscopy (SEM) with energy dispersive spectrometry (EDS), respectively. The inductive coupled plasma atomic emission spectrometer (ICP–AES) was used to examine the percentage composition of each element. The transmission electron microscope (TEM) with electron diffraction was employed to characterize the crystal structure of needle–like precipitates. The mechanical properties of the micro hardness and Young's modulus were characterized by the Leitz micro hardness tester and the tool for Young's modulus, respectively.

1. Introduction

Light metals, often referred to the density which is less than 3.5g·cm^{-3} of metals, including aluminum, magnesium, beryllium and alkali metals. The most representative of light metals are aluminum and magnesium, corresponding to the aluminum and magnesium alloys. Lithium is the lightest alloying element. The density of the aluminum alloy will be reduced by three percent after each one weight percent of the lithium is added [1–3]. Thus, the Al–Li alloys who have low density, high specific strength and high specific stiffness not only can satisfy the requirement of aerospace industry, but also show wide application prospect [3–5]. However, its large–scale application in aerospace industry do not materialize because Al–Li alloys have the disadvantages of low Young's modulus, high toughness, high fracture toughness, low strength, and the high anisotropy of mechanical properties [5]. To solve above problems, rare earth elements were added into Al–Li alloys. Rare earth elements can improve the properties of Al based alloy by forming the Al–RE intermetallic compound and removing the impurities and changing the form of a precipitate during melting processes [5, 6]. Whereas, the Young's modulus and stiffiness of alloy increase a little.

Whisker is a perfect crystal. Researchers have adopted the whisker and fiber of SiC, B_4N, Saffil Al_2O_3 (5% SiO_2 δ–Al_2O_3)

[a] Key Laboratory of Superlight Materials and Surface Technology, Ministry of Education, College of Materials Science and Chemical Engineering, Harbin Engineering University, Harbin 150001, China
[b] Key Discipline Laboratory of Nuclear Safety and Simulation Technology, Harbin Engineering University, Harbin 150001, China
[c] Department of Mechanical Engineering, University of Nevada Las Vegas, Las Vegas, NV 89154−4027, USA

to reinforce the properties of the alloy and make considerable headway [7–10]. However, since the whisker and fiber are adscititious, the binding force with alloy matrix interface is confined. The range of strength has not been enhanced much. Therefore, the opinion that if the whiskers can grow in alloy interior and strengthen the mechanical property of alloy obtained by galvanostatic electrolysis/potentiostatic electrolysis in molten salts attracts our attention. In the electroextraction process of europium in LiCl–KCl–$AlCl_3$–Eu_2O_3, lots of the needle–like precipitates were obtained by Yan et al. [11]. The results from the XRD and SEM show that the needle–like precipitates are Al–Eu intermetallic components. However, further investigation has not been conducted to research whether the needle–like precipitates are whiskers. In addition, to the best of our knowledge, the whiskers prepared by galvanostatic electrolysis/potentiostatic electrolysis in molten salts on liquid cathode have never been reported up till the present moment.

Method of liquid cathode is a process to form alloy with the assistance of liquid metal as cathode. The method can reduce one or more metallic ions from molten salt system to metallic atom by electrode reaction at a relatively positive potential. Adopting this method to manufacture alloy can reduce the activity of alloy, the pollution and loss of dissolution, and electrodeposit high–melting metal to low melting point alloy at a lower temperature. In recent years, the preparation of the alloy and extraction of lanthanides and actinides on the liquid cathode were carried out by many researchers. Castrillejo et al. [12] investigated the electrochemical behavior of praseodymium ions in LiCl–KCl melts on liquid cadmium and bismuth electrodes and successfully prepared various kinds of Pr–Cd and Pr–Bi intermetallic compounds, respectively. Kim et al. [13] represented the electrochemical behavior of the Cerium on solid W and liquid cadmium electrodes and calculated the Gibbs free energies for the formation of Ce–Cd intermetallic compounds. Kim et al. [14] and Koyama et al. [15] investigated the electrochemical behavior of uranium in LiCl–KCl molten salts on liquid cadmium electrode. The results show that the reduction of uranium is one step reaction with a transfer of three electrons on an inert electrode, and the difference of the reduction potential between the inert and liquid cadmium electrode is caused by the activity decrease on the liquid electrode. Under the condition of difference between the reduction potential, the electrorefining uranium on the liquid cadmium electrode was successfully carried out. Our group exihibited the electrochemical behavior of neodymium [16] in NaCl–KCl molten salts on liquid aluminum electrode, and successfully prepared Al–Nd alloys. Based on the literatures mentioned above, all electrochemical behavior and electrolysis experiments were carried out on liquid electrode. However, the information about the preparation of Al–Li–RE alloys containing whiskers on a liquid aluminum electrode in LiCl–KCl melts has never been reported up to now. Therefore, it has great significance to explore the electrochemical behavior of REs and prepare Al–RE intermetallic compound whiskers on liquid aluminum electrode.

Generally speaking, it is difficult to obtain bulk alloy and high reaction rate on solid cathode at a low operation temperature in chloride melts. Moreover, the reaction rate is controlled by the diffusion rate of Lns reduction and the diffusion rate of Lns atoms into aluminum substrate. Therefore, the liquid aluminum at high temperature is selected as the working electrode to prepare the Al–Li–Sm alloy containing whisker. At the same time, the micro hardness and Young's modulus of Al–Li–Sm alloy with and without whiskers were characterized by the Leitz micro hardness tester and the tool for Young's modulus, respectively.

2. Experiment

2.1. Preparation and purification of the melts

The mixture of eutectic LiCl–KCl was first dried under vacuum for more than 48 h at 573 K to remove excess water, and then put into alumina crucible which was placed in an electric furnace. The mass ratio of LiCl–KCl was 1:1. The samarium ions were introduced into the alumina crucible in the form of anhydrous $SmCl_3$ (99.0%) powder. The whole processes of electrochemical measurement and electrolyte were protected by the dry argon atmosphere to avoid the electrolyte contact with oxygen and water. The temperature of the molten salts was monitored by the nickel–chromium thermocouple sheathed with an alumina tube.

2.2. Electrochemical apparatus and electrodes

All electrochemical measurements were accomplished using an Autolab potentiostat/galvanostat, which was controlled by the Nova 1.6 software package. For the measurements of cyclic voltammetry, square wave voltammetry and cathodic polarization curve, the counter electrode was spectral pure graphite rod of 6 mm diameter. A silver wire (d = 1 mm, 99.99% purity) dipped into a solution of AgCl (1 wt. %) in LiCl–KCl eutectic contained in a Pyrex tube was used as the reference electrode. All potentials were referred to this Ag^+/Ag couple. The working electrode was liquid aluminum electrode placed in an alumina crucible. A Mo wire (d=1 mm) which was polished thoroughly using SiC paper and then cleaned ultrasonically with ethanol prior to use placed in the alumina sleeve was immersed in liquid aluminum electrode and used as the electric lead. The active electrode surface area was 1.76 cm^2, which was determined by the cross sectional areas of the alumina crucible and alumina sleeve.

2.3. Preparation and characterization of Al–Li–Sm alloys

The Al–Li–Sm alloy containing whiskers was prepared by the galvanostatic electrolysis at –0.17 $A{\cdot}cm^{-2}$ for 5 hours on liquid aluminum electrode. After the electrolysis, the samples were abraded and polished with 300#, 1500# and 2000# SiC paper followed by ultrasonic cleaning in ethylene glycol and ethanol (99.8% purity) in an ultrasonic bath for 15 min and stored in the glove box until their analysis. The sample was analyzed by the XRD (Rigaku D/max–TTR–III diffractometer) using Cu–Kα radiation at 40 kV and 150 mA. Scanning electron microscopy (SEM) equipped with energy dispersive spectrometry (EDS) (JSM–6480A; JEOL Co., Ltd.) was used to

analyze the microstructure and micro–zone chemical of bulk Al–Li–Sm alloy. To determine the contents of Al, Sm and Li in the sample, the sample was dissolved in aqua regia (HNO_3: HCl: H_2O=1:3:8, v/v). The solution was diluted and analyzed by ICP–AES (Thermo Elemental, IRIS Intrepid II XSP). The crystal structure of the Al–Li–Sm alloy was analyzed by the transmission electron microscopy (JEOL JEM–2010) with electron diffraction. The TEM sample preparation steps were as follows: the samples with thickness of about 0.4 mm were made by line cutting, and then were abraded and polished to about 50 um thickness with 200#, 400# and 1500# SiC paper. After that, the sample was made into circular sheet which diameter was 3 mm, and was thinned by Precision Ion Polishing System (Gatan691). The voltage was 4 kV. The current was 1.5 mA and the angle was –15~15 degree. The whole process of thinning time was 2 h. The Leitz microhardness tester with the conditions of the loading force 200 N and holding pressure time 15 s was used to measure the micro hardness of the alloy. The Young's modulus of alloy was measured by 5077PR square ware pulser Receiver and Tektronix (DPO 3034) oscillograph.

3. Results and discussions

3.1 The electrochemical behavior of Sm (III) on liquid aluminum electrode in LiCl–KCl melts

Cyclic voltammetry

Firstly, the typical cyclic voltammetry was employed to investigate the electrochemical behavior of Sm (III) in chloride melts. Fig. 1 elucidates the cyclic voltammograms in LiCl–KCl melts before (curve 1) and after (curve 2, 3) the addition of 2 wt. % $SmCl_3$ on liquid aluminum electrode at 973 K. Two pairs of redox signals are observed before the addition of $SmCl_3$ (curve 1). At the beginning of the curve 1, an anode signal A' is observed, which is ascribed to the dissolution of liquid aluminum electrode. As the potential goes negative, the reduction signal A at about –0.95 V is related to the reduction of Al(III) ions on the aluminum substrate. The huge cathode signal B at about –2.0 V at the end of the curve 1 is related to the formation of an Al–Li alloy, which is caused by the underpotential deposition of lithium ions on liquid aluminum electrode. In the direction of the anode, an anode signal B' at around –1.35 V is attributed to the dissolution of an Al–Li alloy. After the addition of 2 wt. % $SmCl_3$, a new pair of redox signals between A and B appears. The curve 2 shows the typical cyclic voltammogram obtained in LiCl–KCl–$SmCl_3$ (2 wt. %) melts on liquid aluminum electrode at 973 K. The reduction signal C at around –1.40 V is attributed to the formation of an Al–Sm intermetallic compound. And the anode signal C' between the signals A' and B' at around –1.15 V is related to the dissolution of the Al–Sm intermetallic compound. In order to investigate the corresponding relationship of the cathode/anode signals, the curve 3 was plotted from –0.50 to –1.60 V. It is obvious that the cathode/anode signals B/B' disappear and there are no other cathode/anode signals in the potential range. That is to say, only one kind of Al–Sm intermetallic compound can be formed under our experiment condition. The formation potential of Al–Sm intermetallic compound is more positive than the reduction potential of Sm(II) on an inert electrode. The reason for the potential difference is due to the activity decreasing of the deposited metal in liquid aluminum electrode [17].

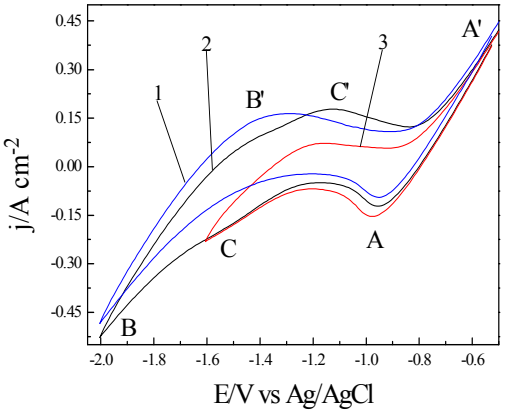

Fig.1 Typical cyclic voltammograms obtained in LiCl–KCl melts before (curve 1) and after (curves 2 and 3) the addition of $SmCl_3$ (2 wt. %) on liquid aluminum electrode (S=1.76 cm^2) at 973 K. Scan rate: 0.1 $V{\cdot}s^{-1}$.

Square wave voltammetry

Square wave voltammetry is a more sensitive method than the cyclic voltammetry. Therefore, the square wave voltammetry was employed to further investigate the electrochemical behavior of Sm(III) on liquid aluminum electrode. Fig. 2 illustrates the square wave voltammograms plotted from –0.90 to –2.0 V in LiCl–KCl melts before (curve 1) and after (curve 2) the addition of 2 wt. % $SmCl_3$ on liquid aluminum electrode at 973 K with the conditions of step potential of 1 mV, frequency of 10 Hz and pulse height of 25 mV. Two reduction signals can be observed (curve 1) before the addition of $SmCl_3$. The first signal A at beginning of the curve 1 is related to the reduction of aluminum ions on an aluminum substrate. The second signal B at the end of the curve is attributed to the formation of an Al–Li alloy, which is formed by the underpotential deposition of lithium on a liquid aluminum electrode. After the addition of 2 wt. % $SmCl_3$ (curve 2) in LiCl–KCl melts on the liquid aluminum electrode at 973 K, a new reduction signal C which begins at –1.07 V and terminates at –1.55 V appears. The reduction signal C is attributed to the formation of an Al–Sm intermetallic compound. The results from the square wave voltammetry are in accord with the results from the cyclic voltammetry.

Cathodic Polarization test

The cathodic polarization curve with low scan rate is a steady–state process, and is an excellent method to investigate the formation of alloys. Thus, the cathodic polarization curve was used to verify the results from the cyclic voltammetry and the square wave voltammetry. Fig. 3 illustrates the cathodic

polarization curve obtained in LiCl–KCl melts after the addition of 2 wt. % $SmCl_3$ on liquid aluminum electrode at 973 K. The scan rate is 5 $mV \cdot s^{-1}$. At the beginning of the curve, the signal A′ is related to the oxidation process of metal aluminum. When the potential reaches about –0.76 V, the signal A is ascribed to the reduction of Al(III). With the potential goes to –1.23 V, the first turning point C can be observed. The turning point C corresponds to the formation of an Al–Sm intermetallic compound. The last turning point B is ascribed to the formation of an Al–Li alloy, which is formed by the underpotential deposition of lithium ions on liquid aluminum electrode. The results from the polarization test are consistent with the results from the cyclic voltammetry and the square wave voltammetry.

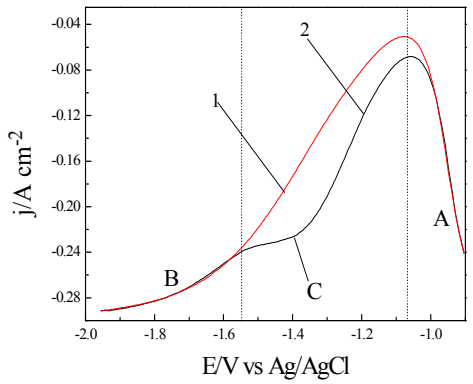

Fig. 2 Square wave voltammograms of LiCl–KCl melts before (curve 1) and after (curve 2) the addition of $SmCl_3$ (2 wt. %) on liquid aluminum electrode (S=1.76 cm^2) at 973 K. Pulse height: 25 mV; potential step: 1 mV; frequency: 10 Hz.

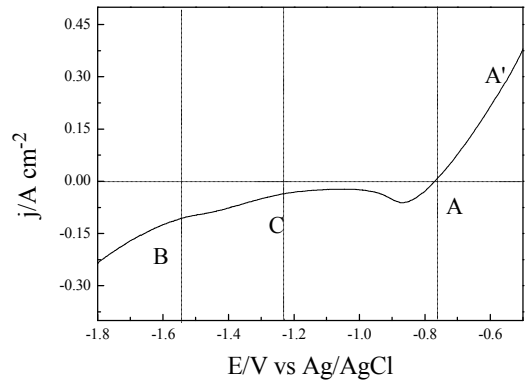

Fig. 3 Cathodic polarization curve of the LiCl–KCl melts before and after the addition of $SmCl_3$ (2 wt. %) on liquid aluminum electrode (S=1.76 cm^2) at 973 K (scan rate: 5 $mV \cdot s^{-1}$).

3.2 Preparation and characterization of Al–Li–Sm alloys containing whiskers in LiCl–KCl–$SmCl_3$ melts at 973 K on the liquid aluminum electrode

Based on above electrochemical results, galvanostatic electrolysis was carried out to prepare Al–Li–Sm alloy containing whiskers on liquid aluminum electrode. In this way, galvanostatic electrolysis was applied for a given time, and then it was interrupted. After electrolysis, the alloy was kept in the melt and gradually cooled to the room temperature (cooling rate is 2 ^oC/min). To avoid the electrolyte contacting with oxygen and water, the whole process was protected with the argon atmosphere. Then, the alloy was separated from the melts and stored inside the glove box until analysis.

Fig. 4 formulates the typical evolution of cathodic potentials during galvanostatic electrolysis in LiCl–KCl melts after the addition of 10 wt. % $SmCl_3$ on liquid aluminum electrode at 973 K, the current density is –0.17 $A \cdot cm^{-2}$. In the electrolysis process, the electrolytic potential is no more than –1.825 V. In other words, there is a small amount of lithium deposition on liquid aluminum electrode. Fig. 5 illustrates the XRD pattern of Al–Li–Sm alloy obtained on the liquid aluminum electrode in LiCl–KCl–$SmCl_3$ (10 wt. %) melts at 973 K after galvanostatic electrolysis for 5 hours. It is easy to find that the Al–Li–Sm alloy mainly contains Al_4Sm and Al phases. Twelve XRD diffraction peaks corresponding to Al_4Sm intermetallic compound can be obtained from Fig. 5. By comparing them with the JCPDS of Al_4Sm in the XRD data bases, the values are obtained and listed in Table 1. The theta values corresponding to the diffraction peaks are nearly the same. It is worthwhile to note that there are no diffraction peaks of Al–Li intermetallic compounds. The phenomenon may be caused by two reasons. One is that the chemical affinity of Al–Sm is higher than that of Al−Li. Another probability is that the lithium content of alloy is low. Thus, the ICP was used to examine the percentage composition of each element. The result from the ICP shows that the compositions of alloy include 1.5 wt. % Li, 7.9 wt. % Sm and 90.6 wt. % Al. The SEM with EDS map analysis was employed to investigate the surface morphology of the alloy. Fig. 6 illustrates the SEM with EDS map analysis of Al–Li–Sm alloy obtained on a liquid aluminum electrode (S=1.76 cm^2) in LiCl–KCl–(10 wt. %) $SmCl_3$ melts after galvanostatic electrolysis for 5 hours at 973 K. From the SEM image, it can clearly be seen that a lot of needle–like precipitates form in Al–Li–Sm alloy, and the ratio of length to diameter of the needle–like precipitates is greater than 10:1. The EDS map analysis was employed to investigate the distribution of the elements. The results from the EDS map analysis indicate that the samarium element mainly distributes in needle–like precipitates and the aluminum element mainly distributes on the grey area. In order to further investigate the situation of the element distribution, the EDS quantitative analysis of Al–Li–Sm alloy was employed. Fig. 7 shows the SEM with EDS quantitative analysis of the Al–Li–Sm alloy. The points 1 and 2 locate on the needle–like precipitates and the point 3 locates on the grey area. The EDS results of the points labeled 1 and 2 taken from needle–like precipitates indicate that the deposit is composed of elements Al and Sm.

Table 1

Comparison of JCPDS of Al_4Sm in the XRD data bases and present work values

	Standard	Present work
2Theta	17.96	17.71
	22.68	22.47
	29.59	29.51
	34.68	34.58
	36.31	36.02
	42.13	42.17
	48.30	48.30
	50.69	50.50
	55.57	55.45
	64.29	64.03
	68.11	68.00
	72.27	72.21

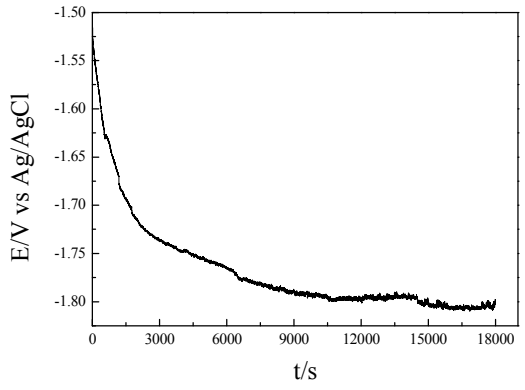

Fig. 4 Typical evolution of cathodic potentials during galvanostatic electrolysis in LiCl–KCl melts after the addition of 10 wt. % $SmCl_3$ on liquid aluminum electrode at 973 K, current density is –0.17 $A \cdot cm^{-2}$.

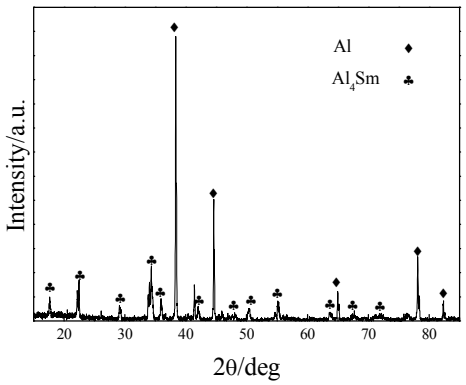

Fig. 5 XRD pattern of Al–Li–Sm alloy obtained on liquid aluminum electrode (S=1.76 cm^2) in LiCl–KCl melts after the addition of 10 wt. % $SmCl_3$ at 973 K.

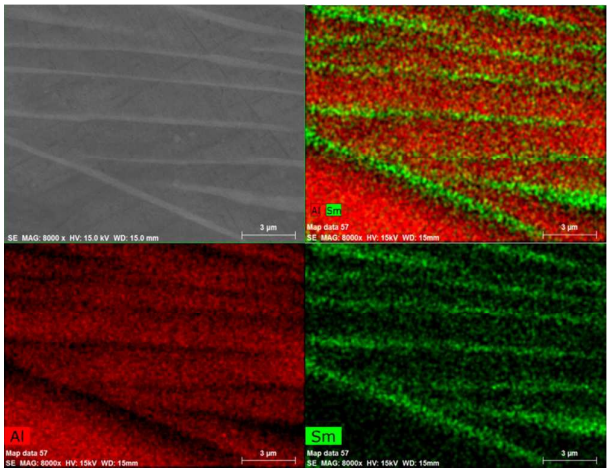

Fig. 6 The SEM with EDS map analysis of Al–Li–Sm alloy obtained on liquid aluminum electrode (S=1.76 cm^2) in LiCl–KCl melts after the addition of 10 wt. % $SmCl_3$ at 973 K.

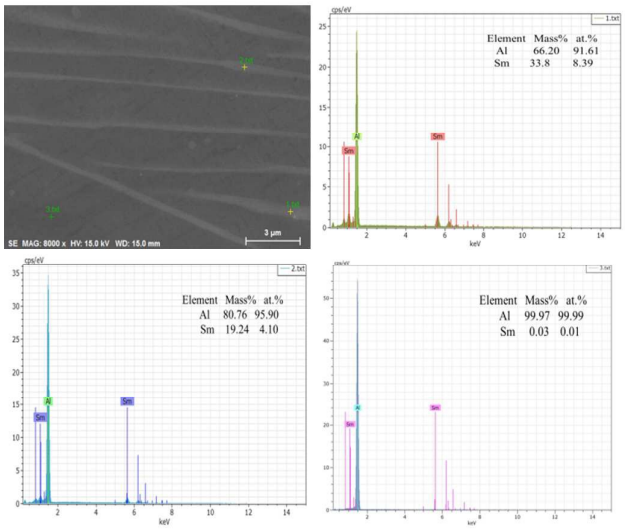

Fig. 7 The SEM with EDS quantitative analysis of Al–Li–Sm alloy obtained on liquid aluminum electrode (S=1.76 cm^2) in LiCl–KCl melts after the addition of 10 wt. % $SmCl_3$ at 973 K.

As long as the single crystal structure is met and the ratio of length to diameter is greater than 10 to 1, it can be concluded that it is whisker. From the SEM images, it is obvious that the ratio of length to diameter of the needle–like precipitates is greater than 10:1. Therefore, it is important to verify whether the needle–like precipitate is single crystal structure. Thus, the transmission electron microscope with electron diffraction test was adopted to research the crystal structure of the needle–like precipitate. Fig. 8 shows the TEM image (a), EDS analysis (b) and electron diffraction pattern (c) of Al–Li–Sm alloy containing whiskers obtained by galvanostatic electrolysis for 5 hours at 973 K on a liquid aluminum electrode in the LiCl–KCl–$SmCl_3$ (10 wt. %) melts. From the TEM image (Fig. 8a), the needle–like precipitate can be also observed in the alloy. Fig. 8b illustrates the EDS/TEM analysis of the needle–like precipitate. It is easy to find that the needle–like precipitate is composed of

elements Al and Sm. Then, the point A was taken from random area of the needle–like precipitate, and the electron diffraction image (Fig. 8c) was obtained. The result from the electron diffraction image shows that the diffraction spots arranged in an orderly manner. Thus, the crystal structure of needle–like precipitate is single–crystal structure. Combining the above results of the SEM&EDS and TEM&EDS, the needle–like precipitates can be regarded as the Al–Sm intermetallic compound whiskers.

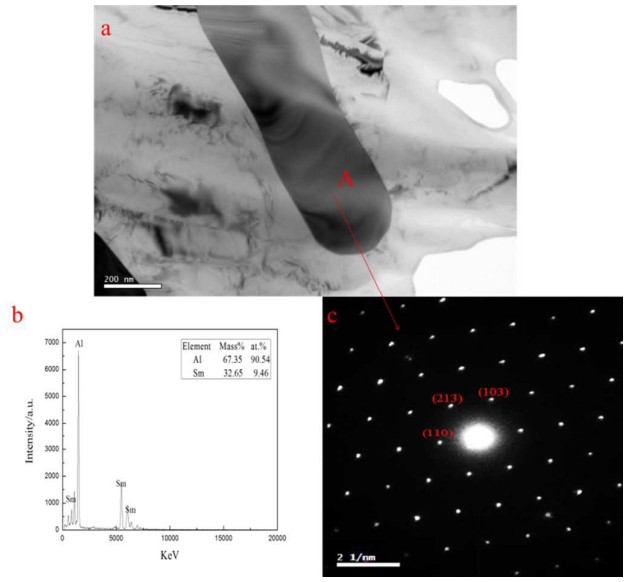

Fig. 8 TEM image (a), EDS analysis (b) and electron diffraction pattern (c) of Al–Li–Sm alloy containing whiskers obtained by galvanostatic electrolysis for 5 hours at 973 K on a liquid aluminum electrode in LiCl–KCl–$SmCl_3$ (10 wt. %) melts.

3.3 The test of mechanical properties

Micro hardness

The purpose of synthetic Al–Li–Sm alloy containing whiskers is mainly to verify whether the whiskers can improve the mechanical properties of the alloy. Thus, the Leitz micro hardness tester was used to measure the micro hardness of the alloy. First, the two kinds of alloys with nearly the same composition of Al, Li and Sm were prepared under the same experiment condition. However, the cooling rate of preparing these two kinds of Al–Li–Sm alloy is different. The cooling rate of Al–Li–Sm alloy containing whiskers was 2 ^{o}C/min, but Al–Li–Sm alloy without whiskers was separated from the melts and directly cooled to the room temperature after galvanostatic electrolysis for 5 h with the protection of argon atmosphere. Then, a series of experiments of hardness test were completed by the micro hardness tester. Fig. 9 illustrates the comparison diagram of micro hardness of Al−Li−Sm alloy with (column chart 1) and without whiskers (columu chart 2). The column chart 1 illustrates the micro hardness of the Al–Li–Sm alloy containing whiskers obtained by galvanostatic electrolysis for 5 hours at 973 K on the liquid aluminum electrode in LiCl–KCl–$SmCl_3$ (10 wt. %) melts. From the column chart 1, micro hardness of the Al–Li–Sm alloy containing whiskers can be identified as 63.6±0.8 HV. The column chart 2 shows the micro hardness of the Al–Li–Sm alloy without whiskers. The micro hardness from the column chart 2 is 54.3±0.6 HV. It is easy to find that micro hardness of Al–Li–Sm alloy containing whiskers improves 17.1% in comparison with Al–Li–Sm alloy without whiskers.

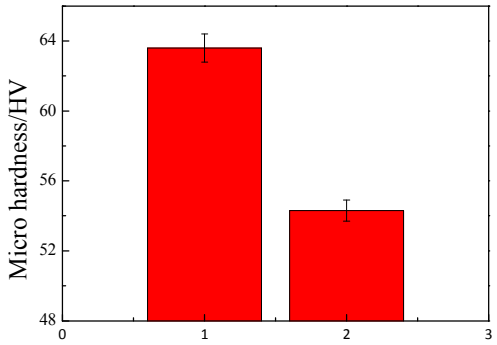

Fig. 9 The comparison diagram of micro hardness of Al–Li–Sm alloy with (column chart 1) and without whiskers (columu chart 2).

Young's modulus

In order to further investigate the mechanical property of Al–Li–Sm alloy containing whispers, the elasticity modulus of the alloy was measured by measuring instrument of Young's modulus. The Young's modulus was calculated using following formula [18]:

$$E = \frac{V_L^{\,2}\rho(1+\nu)(1-2\nu)}{(1-\nu)}$$

Where E is Young's modulus, ν is Poisson's ratio, ρ is the density of the Al–Li–Sm alloy and V_L is the propagation speed of longitudinal waves. The density of the alloy was measured by drainage. The Poisson's ratio was calculated by the following equation [18]:

$$\nu = \frac{1-2(V_T - V_L)^2}{2-2(V_T - V_L)^2}$$

Where V_T is the velocity of the transverse waves. The propagation speed of longitudinal waves and the velocity of the transverse waves can be calculated by the wave length of longitudinal and transverse waves and the time of propagation. Fig. 10 exhibits the comparison diagram of Young's modulus of Al–Li–Sm alloy with (column chart 1) and without whiskers (columu chart 2). The Young's modulus values of Al–Li–Sm alloys with and without whiskers are 80.54 ± 0.54 GPa and 77.44 ± 0.38 GPa, respectively. It is obvious that Young's modulus of Al–Li–Sm alloy containing whiskers improves 4% in comparison with Al–Li–Sm alloy without whiskers.

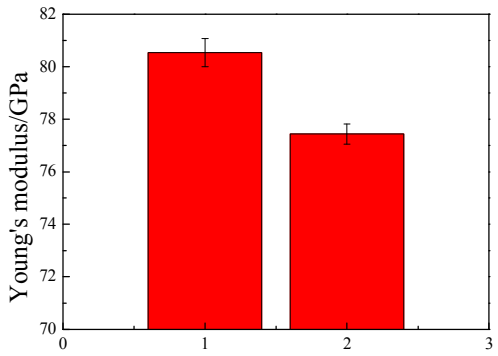

Fig. 10 Comparison diagram of the Young's modulus of Al–Li–Sm alloy with (column chart 1) and without whiskers (columu chart 2).

Conclusions

The electrochemical behavior of samarium ions on liquid aluminum electrode in LiCl–KCl melts was investigated by different electrochemical measurements. Only one kind of Al–Sm intermetallic compound (Al_4Sm) can be formed under the Al–rich experiment condition. XRD result of Al–Sm alloy containing whiskers obtained by galvanostatic electrolysis in LiCl–KCl–$SmCl_3$ (10 wt. %) melts on liquid aluminum electrode illustrates that Al_4Sm phase is formed. The SEM shows that many needle–like precipitates form on the surface of the aluminum substrate, and these precipitates are finally identified as Al–Sm intermetallic compound whiskers by TEM with electron diffraction test. Both elastic modulus and micro hardness of Al–Li–Sm alloy containing whiskers are further improved. The micro hardness and Young's modulus of Al–Li–Sm alloy containing whiskers improve 17.1% and 4% in comparison with the Al–Li–Sm alloy without whiskers, respectively.

Acknowledgements

The work was financially supported by the China Scholarship Council, the National Natural Science Foundation of China (21103033, 21101040, 91226201 and 51574097), the Fundamental Research funds for the Central Universities (HEUCF20151007), the Foundation for University Key Teacher of Heilongjiang Province of China and Harbin Engineering University (1253G016 and HEUCFQ1415), and the Special Foundation Heilongjiang Postdoctoral Science Foundation (LBH–TZ0411).

References

[1]E. J. Lavernia, T. S. Srivatsan and F. A. Mohamed, *J. Mater. Sci.*, 1990, **25**, 1137−1158.
[2]C. H. Joh, K. Yamada and Y. Miura, *Mater. Trans.*, 1999, **40**, 439−442.
[3]R. K. Gupta, N. Nayan, G. Nagasireesha and S. C. Sharma, *Mater. Sci. Eng.*, 2006, **420**, 228−234.
[4]T. Kaminski, E. Willner, J. Kerr and H. Taketani, *DGM Metallurgy Information*, 1992, **2**, 1311−1316.
[5]L. Meng and X. L. Zheng, *Mater. Sci. Eng.*, 1997, **237**, 109−118.
[6]K.S. Kumar and F.H. Heubaum, *Acta Mater.*, 1997, **45**, 2317−2327.
[7]D. G. Gonzalez, J. Wolfenstine and P. Metenier, *J. Mater. Sci.*, 1990, **25**, 4535−4540.
[8]J. Wolfenstine, D. G. Gonzalez and O. D. Sherby, *Mater. Lett.*, 1992, **15**, 305−308.
[9]C.J. Ma, D. Zhang and J.N. Qin, *J. Rare Metals*, 1999, **23**, 401−404.
[10]J. F. Mason, C. M. Warwick and P. J. Smith, *J. Mater. Sci.*, 1989, **24**, 3934−3946.
[11]Y. D. Yan, H. Tang, M. L. Zhang, Y. Xue, W. Han, D. X. Cao and Z. J. Zhang, *Electrochim. Acta*, 2012, **59**, 531−537.
[12]Y. Castrillejo, M. R. Bermejo and P. DíazArocas, *J. Electroanal. Chem.*, 2005, **579**, 343−358.
[13]S.H. Kim, S. Paek, T.J. Kim, D.Y. Park and D.H. Ahn, *Electrochim. Acta*, 2012, **85**, 332−335.
[14]G.Y. Kim, D. Yoon, S. Paek, S.H. Kim, T.J. Kim and D.H. Ahn, *J. Electroanal. Chemi.*, 2012, **682**, 128−135.
[15]T. Koyama, M. IIzuka, Y. Shoji, R. Fujita, H. Tanaka, T. Kobayashiz and M. Tokiwai, *J. Nucl. Sci. Technol.*, 1997, **4**, 384−393.
[16]X. Li, Y. D. Yan, M. L. Zhang, Y. Xue, H. Tang, D. B. Ji and Z. J. Zhang, *RSC Adv.*, 2014, **4**, 40352−40358.
[17]M. Kurata, Y. Sakamura and T. Matsui, *J. Alloys Compd.*, 1996, **234**, 83−92.
[18]L.L. Chapelon, J. Vitiello, D. Neira, J. Torres, J.C. Royer, D. Barbier, F. Naudin, G. Tas, P. Mukundhan and J. Clerico, *Microelectron. Eng.*, 2006, **83**, 2346−2350.

A graphical abstract

TEM image and electron diffraction pattern of Al–Li–Sm alloy containing whiskers obtained by galvanostatic electrolysis.